PAPER

Cascaded semiconductor optical amplifiers-based all-optical OR logic gate

Physica Scripta

PAPER

Cascaded semiconductor optical amplifiers-based all-optical OR logic gate

RECEIVED
9 November 2020

REVISED
18 March 2021

ACCEPTED FOR PUBLICATION
24 March 2021

PUBLISHED
1 April 2021

Amer Kotb[1,2], **Kyriakos E Zoiros**[3] **and Wei Li**[1]

[1] GPL, State Key Laboratory of Applied Optics, Changchun Institute of Optics, Fine Mechanics and Physics, Chinese Academy of Sciences, Changchun 130033, People's Republic of China
[2] Department of Physics, Faculty of Science, University of Fayoum, Fayoum 63514, Egypt
[3] Lightwave Communications Research Group, Department of Electrical and Computer Engineering, School of Engineering, Democritus University of Thrace, Xanthi 67100, Greece

E-mail: amer@ciomp.ac.cn **and** weili1@ciomp.ac.cn

Keywords: all-optical OR logic gate, cascaded semiconductor optical amplifiers, quality factor

Abstract

We present a novel study of the ultrafast performance of an all-optical OR logic gate using two-cascaded semiconductor optical amplifiers (SOAs) at a data rate of 80 Gb s^{-1}. The variation of the gate's quality factor (Q-factor) against various key operating parameters, such as the continuous wave input power and wavelength, the operating data rate and the equivalent pseudorandom binary sequence length, is examined and assessed, taking into account the effects of SOAs amplified spontaneous emission and operating temperature to obtain results that are closer to reality. The simulation results indicate that the OR logic gate can be realized using the proposed two-cascaded SOAs scheme at 80 Gb s^{-1} with logical correctness and a Q-factor $=$ 23.7, which is higher than that previously reported with other SOA-based schemes.

1. Introduction

All-optical (AO) signal processing has been proposed as an efficient means for avoiding cumbersome optoelectronic conversions in modern ultra-high speed optical networks and systems. AO logic gates are fundamental modules for realizing AO signal processing functionalities and applications [1, 2]. The OR is one such basic logic gate. On the other hand, Semiconductor Optical Amplifiers (SOAs) have distinctive features over other technologies, such as the compact size, the wide bandwidth, the low power consumption and the ease of integration with other optoelectronic devices. These unique characteristics have rendered SOAs the primary choice as nonlinear elements for the implementation of different AO logic gates. In particular, the OR gate has been implemented using SOAs assisted by different interferometers, such as the Delayed Interferometer (DI) [3] and the Mach–Zehnder Interferometer (MZI) [4, 5]. Although these schemes have shown some advantages in terms of small pattern dependence and reduced operating requirements, yet they are difficult to control or construct, while random phase changes are critical to their performance. Thus, in this paper, we show that two-cascaded SOAs, which are more straightforward and flexible to operate and optimize, can be used to realize an AO OR logic gate at 80 Gb s^{-1} with better performance and higher quality factor (Q-factor) than previously reported [3–6]. Various other logic gates have been realized using two-cascaded SOAs, for example, a logic XOR gate [7], logic AND gate [8, 9] and logic NOR gate [9, 10]. The novelty of this research lies in the continuity as well as the extension of the previous relevant works on two-cascaded SOAs-based logic gates [7–10] by numerically studying, for the first time to our knowledge, the OR operation. To verify whether the performance of the considered Boolean function is acceptable and even comparatively better when using for this purpose two-cascaded SOAs, we examine and assess the effect of the SOAs' and input signals' key operating parameters on the gate's Q-factor, including the effects of the amplified spontaneous emission (ASE) noise and operating temperature (T_{OP}) for a more realistic simulation.

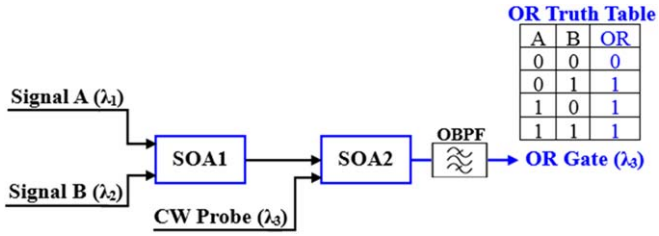

Figure 1. Schematic diagram and truth table of OR operation using two-cascaded SOAs. CW: continuous wave. OBPF: optical bandpass filter.

2. OR gate using cascaded SOAs

2.1. Operation principle

The schematic diagram and truth table of the AO OR logic gate using two-cascaded SOAs is shown in figure 1. Two required steps are involved to perform the OR operation using two-cascaded SOAs. At the first step, signal A at wavelength λ_1 and signal B at wavelength λ_2 are launched into SOA1. Then, during the second step, a continuous wave (CW) beam at a different wavelength λ_3 is injected into SOA2 together with the outcome of SOA1. The operation of the circuit relies on self-gain modulation (SGM) in SOA1 [11] and cross-gain modulation (XGM) in SOA2 [12]. More specifically, SGM is an effect that corresponds to the modulation of the SOA gain induced by the variation of the power of the input signal itself. XGM is a nonlinear effect similar to SGM, but the modulation of the SOA gain, which is induced by a strong optical signal, known as 'control' or 'pump', affects the gain of another weak signal, known as the 'probe', propagating simultaneously in the SOA. The common characteristic of both SGM and XGM which is exploited in the context of all-optical switching is that higher level signals experience lower SOA gain than lower level signals [13], with the difference of course that in SGM this change is reflected on the single signal exiting the SOA, while in XGM it is imprinted on the secondary, or auxiliary, signal (the probe) that finally emerges at the SOA output. Now in our case, data signals A and B, which are pulsed, occupy a defined fraction of their allocated bit slot and pursued to execute all-optically the Boolean OR logic between them, are initially launched into SOA1 to determine its output based on SGM according to the following binary combinations: When A = '1' and B = '0', signal A reduces SOA1 gain, while signal B does not affect it, thus the level of the outcome is low or equivalent to '0'. The same happens for A = '0' and B = '1'. When A = '1' and B = '1', SOA1 gain is also dropped to an extent that the level of the product is also low, or '0' again. Provided that signals A and B are strong enough, SOA1 will be heavily saturated by the same degree no matter whether A and B act separately or simultaneously on this active device. This is a necessary requirement that must be satisfied for SOA1 response to A and B pairs different than all '0' to be uniform. Another operating requirement concerns the fact that the wavelengths of A and B should not be located far away from each other, first so that both lie within SOA1 3 dB gain bandwidth, and second so that they encounter identical SOA1 optical and material properties. The resultant signal is forwarded as a pump to SOA2, which is concurrently driven by the CW beam as the probe. Then subject to the manifestation of XGM, SOA2 gain will be recovering away from saturation for the three out of the four logic possibilities that at least one of signals A or B is different than '0'. When mapped on the CW beam transferred at SOA2 output and selected by an optical bandpass filter (OBPF) that rejects the co-propagating pump, this will be translated into a high level outcome, or '1'. In contrast, SOA2 will receive from SOA1 a strong signal enabled by SOA1 unperturbed gain due to the absence of both A and B (= '0'). Thus SOA2 gain will heavily decline and accordingly experienced by the CW beam as a low level, or '0', which will eventually emerge at SOA2 output. In this manner, SOA2 gain modulation depends on that of SOA1, which in turn is governed by the logic combination of data A, B. Through this physical interaction, SOA2 produces the logic conjugate of SOA1, which corresponds to the truth table of the OR gate. Note that the Cross Phase Modulation (XPM) effect, which consists in SOA refractive index changes induced by one optical signal and affecting the output phase of all other signals propagating along with the SOA, is not exploited here, as is not necessary, but it would instead be useful in the context of interferometric-based all-optical switching for Boolean logic purposes, as in [14].

2.2. Numerical analysis

The intraband effects of carrier heating (CH) and spectral hole burning (SHB) manifest inside SOAs driven by high intensity and narrow width input signals [15]. These processes occur in a very short time scale of a few picoseconds, therefore their influence should be taken into account, together with the interband effect of carrier depletion (CD), when seeking to provide an accurate numerical model of SOAs dynamic behavior. Then the

time-dependent gain of each SOA is described by the following set of first-order differential equations [4, 16]:

$$\frac{dh_{CD}(t)}{dt} = \frac{h_0 - h_{CD}(t)}{\tau_C} - (\exp[h_{CD}(t) + h_{CH}(t) + h_{SHB}(t)] - 1)\frac{P_{in}(t)}{E_{sat}} \tag{1}$$

$$\frac{dh_{CH}(t)}{dt} = -\frac{h_{CH}(t)}{\tau_{CH}} - \frac{\varepsilon_{CH}}{\tau_{CH}}(\exp[h_{CD}(t) + h_{CH}(t) + h_{SHB}(t)] - 1)P_{in}(t) \tag{2}$$

$$\frac{dh_{SHB}(t)}{dt} = -\frac{h_{SHB}(t)}{\tau_{SHB}} - \frac{\varepsilon_{SHB}}{\tau_{SHB}}(\exp[h_{CD}(t) + h_{CH}(t) + h_{SHB}(t)] - 1)P_{in}(t) - \frac{dh_{CD}(t)}{dt} - \frac{dh_{CH}(t)}{dt} \tag{3}$$

where factors 'h' symbolize the SOAs's gain integrated over their length due to CD (h_{CD}), CH (h_{CH}) and SHB (h_{SHB}). $G_0 = \exp[h_0]$, where G_0 is the unsaturated power gain given by $G_0 = a\Gamma(I\tau_c/eV - N_{tr})L$ [16], where a is the differential gain, Γ is the optical confinement factor, I is the injection forward current, τ_c is the carrier lifetime, e is the electron charge, $V = wdL$ is the active layer volume, N_{tr} is the transparency carrier density and L is the active region length. E_{sat} is the saturation energy given by $E_{sat} = P_{sat}\tau_c = wdhf/a\Gamma$ [16], where P_{sat} is the saturation power, w & d are the width and thickens of the active layer, respectively, h is the Planck's constant and hf is the photon energy. τ_{CH} and τ_{SHB} are, respectively, the temperature relaxation rates due to CH and SHB. ε_{CH} and ε_{SHB} are, respectively, the nonlinear gain suppression factors due to CH and SHB. $P_{in}(t)$ is the total input power of either SOA1 or SOA2. The input data A and B are assumed to be Gaussian-shaped return-to-zero pulses having energy E_0, full-width at half-maximum pulse width τ_{FWHM} and period T, which is the inverse of the operating data rate, i.e. [16]:

$$P_{A,B}(t) \equiv P_{in}(t) = \sum_{n=1}^{N} a_{n(A,B)} \frac{2\sqrt{\ln[2]}\,E_0}{\sqrt{\pi}\,\tau_{FWHM}} . \exp\left[-\frac{4\ln[2](t - nT)^2}{\tau_{FWHM}^2}\right] \tag{4}$$

where $\alpha_{n(A,B)}$ denotes the binary content of the n-th bit slot in data streams A and B, i.e. $\alpha_{n(A,B)}$ = '1' or '0', which are contained within pseudorandom binary sequences (PRBS) of length $N = 2^7 - 1$ [4].

Then the total gain of each SOA is given by [4, 16]:

$$G_{SOA_i}(t) = \exp[h_{CD}(t) + h_{CH}(t) + h_{SHB}(t)],\ i = 1, 2 \tag{5}$$

The phase change induced inside each SOA is given by [4, 16]:

$$\Phi_{SOA_i}(t) = -0.5(\alpha\, h_{CD}(t) + \alpha_{CH} h_{CH}(t)), \quad i = 1, 2 \tag{6}$$

where α is the traditional linewidth enhancement factor, namely α-factor and α_{CH} is the linewidth enhancement factor due to CH. Note that the corresponding contribution of SHB is null, i.e. $\alpha_{SHB} = 0$ [4].

According to figure 1, the input optical powers going inside SOA1 and SOA2 during the two operating steps taken to perform the OR operation using two-cascaded SOAs are, respectively, expressed by:

$$P_{in,\,SOA_1}(t) = P_A(t) + P_B(t) \tag{7}$$

$$P_{in,\,SOA_2}(t) = P_{out,\,SOA_1}(t) + P_{CW} \tag{8}$$

The complex electric field emerging from SOA1 is given by [17]:

$$E_{out,\,SOA_1}(t) = \sqrt{P_{in,\,SOA_1}(t)}\exp[0.5\ln[G_{SOA_1}(t)] + j\,\Phi_{SOA_1}(t)] \tag{9}$$

while the complex electric field of the signal coming out of SOA2 is given by:

$$E_{out,\,SOA_2}(t) = \sqrt{P_{in,\,SOA_2}}\exp[0.5\ln[G_{SOA_2}(t)] + j\,\Phi_{SOA_2}(t)] \tag{10}$$

where $G_{SOA1,2}(t)$ and $\Phi_{SOA1,2}(t)$ are the total gains and phase shifts of SOA1 and SOA2, respectively. *j* denotes the imaginary part.

The OBPF is assumed to exhibit a Gaussian-shaped response whose field transfer function in the frequency domain is given by [17]:

$$OBPF(f) = \exp\left[-\ln[\sqrt{2}]\left(\frac{f - f_c}{B_f/2}\right)^{2M}\right] \tag{11}$$

where f_c is the filter's center frequency and B_f is the filter's optical bandwidth. M is the filter's order, which determines the sharpness of the filter's passband edges, i.e. $M = 1$ corresponds to Gaussian and $M \geqslant 2$ to super-Gaussian shapes. Now, since SOA2 is connected to the OBPF, the OR output power coming out of the OBPF is analogous to the square modulus of the filter's output electric field, i.e. [17]:

$$P_{out,OR}(t) = |E_{OBPF}(t)|^2 = |F^{-1}[F[E_{out,SOA_2}(t)] \cdot OBPF(f)]|^2 \tag{12}$$

where operators F and F^{-1} denote the fast Fourier transform and its inverse, respectively.

Table 1. OR default parameter values [1–18].

Symbol	Definition	Value	Unit
E_0	Pulse energy	0.1	pJ
τ_{FWHM}	Pulse width	1	ps
T	Bit period	12.5	ps
N	PRBS length	127	—
λ_1	Wavelength of signal A	1559	nm
λ_2	Wavelength of signal B	1546	nm
λ_3	Wavelength of CW beam	1554	nm
I	Injection current	180	mA
P_{sat}	Saturation power	30	mW
τ_c	Carrier lifetime	25	ps
α	α-factor	5	—
N_{tr}	Transparency carrier density	10^{24}	m^{-3}
α_{CH}	CH linewidth enhancement factor	1	
α_{SHB}	SHB linewidth enhancement factor	0	
ε_{CH}	CH Nonlinear gain suppression factor	0.02	W^{-1}
ε_{SHB}	SHB Nonlinear gain suppression factor	0.02	W^{-1}
τ_{CH}	Temperature relaxation rate	0.3	ps
τ_{SHB}	Carrier-carrier scattering rate	0.1	ps
Γ	Optical confinement factor	0.3	—
a	Differential gain	2×10^{-16}	cm^2
L	Length of active layer	0.5	mm
d	Thickness of active layer	0.3	μm
w	Width of active layer	3	μm
G_0	Unsaturated power gain	30	dB
N_{SP}	Spontaneous emission factor	2	
T_{OP}	Operating temperature	290	K
m_0	Free electron mass	9.109×10^{-31}	kg
h	Planck's constant	6.63×10^{-34}	J·s
k	Boltzmann's constant	1.38×10^{-23}	$J \cdot K^{-1}$
f_c	Filter's center frequency	193.1	THz
B_f	Filter's optical bandwidth	1.6	THz
M	Filter's order	2	—

To evaluate the performance of the considered gate using the proposed scheme, the Q-factor is employed as the most appropriate metric to characterize the quality of the output signals. This metric is defined as the ratio of the mean peak powers of '1' and '0' bits, P_1 and P_0, to the corresponding standard deviations, σ_1 and σ_0, respectively, i.e. Q-factor $= (P_1 - P_0)/(\sigma_1 + \sigma_0)$ [16]. The value of the Q-factor must exceed 6 to ensure that the logic gate performance is acceptable, as it guarantees that the related bit-error-rate [18] is kept below 10^{-9} [7]. The SOAs' response equations (1)–(3) are solved using Adam's numerical method run in Wolfram Mathematica® for the default parameters values cited in table 1 [1–18]. It should be noted here that these parameters values are in line with cited publications that have used SOAs with similar optical and physical characteristics. Here we have also tried to use relevant parameter values which are compatible with those of practical SOAs (for instance as those of Inphenix Model IPSAD 1501, with 25 ps carrier recovery time [7]).

3. Results and discussion

Figure 2 shows the simulation results of the AO OR logic gate between representative pattern segments of data signals A and B using two-cascaded SOAs at 80 Gb s^{-1}. The pseudo-eye diagram is clear, open and uniform. It is supported by a Q-factor $= 23.7$, which is more acceptable than when using a conventional SOA-followed by a DI [3] or SOAs-MZI [4] to achieve OR operation at the same data rate. Furthermore, the OR gate is executed with logical correctness in accordance with its truth table.

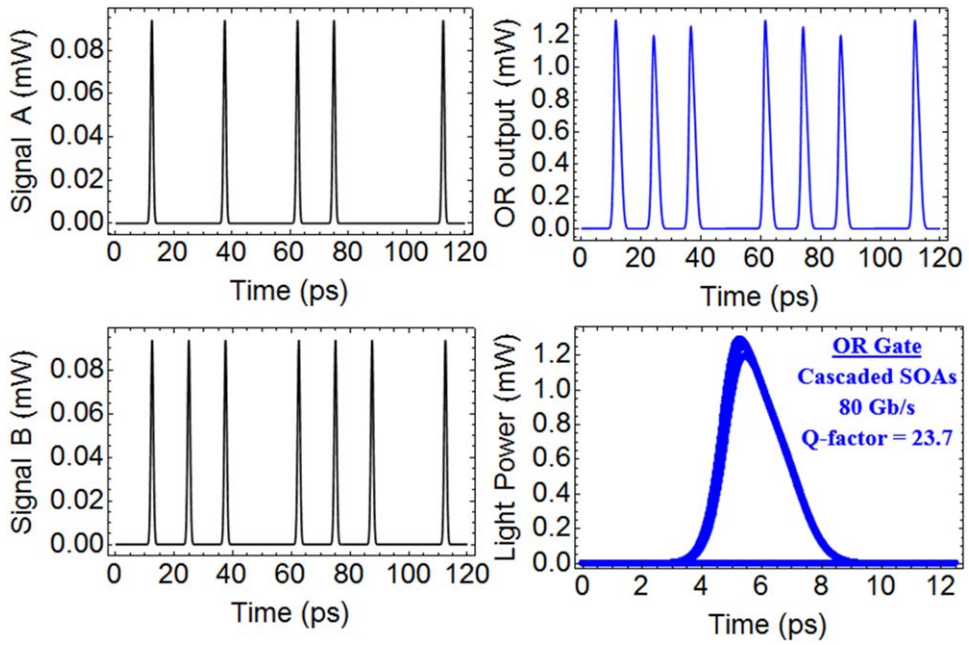

Figure 2. Simulation results of OR gate using two cascaded SOAs at 80 Gb s^{-1}.

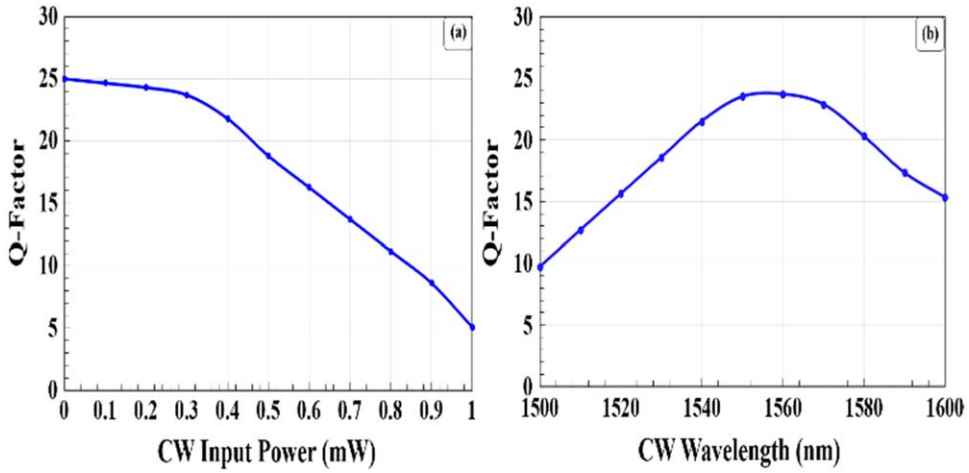

Figure 3. Q-factor of OR gate using two-cascaded SOAs at 80 Gb s^{-1} versus CW beam (a) input power and (a) wavelength.

The AO OR gate operation depends on the characteristics of the incident CW signal. Therefore, we examined the effect of the CW beam power and wavelength on the output Q-factor of the OR gate using two-cascaded SOAs at 80 Gb s^{-1}, as shown in figures 3(a) and (b), respectively. From figure 3(a) it can be seen that the CW power should not exceed a certain threshold up to which the Q-factor remains very high and also quite insensitive to its variations. Beyond this point, which appears as a knee in the curve, the Q-factor starts to decline sharply. This happens because then the CW power becomes such that the CW beam no longer acts as the probe but dominates the SOA2 gain dynamics, thus masking the pump-like role of SOA1 output going into SOA2. On the other hand, from figure 3(b) it appears that the wavelength of the CW light is not so critical provided that it lies between the 1550 nm to 1570 nm band. This ensures that the Q-factor remains quite insensitive to changes of this parameter inside the specified range, while it is also much higher than its values at the extremes of the examined span.

It is also important to examine the gate's performance against the operating data rate and equivalent PRBS length. This is shown in figure 4. More specifically, figure 4(a) shows that although the Q-factor is decreased as data arrive more often and compromise the SOAs capability to timely handle them, still the proposed scheme manages to achieve a more than acceptable Q-factor $=$ 9.2 up to 240 Gb s^{-1}. This speed seems to be possible due to the combined use of very short optical data pulses and CW beam, which both help accelerate the SOAs

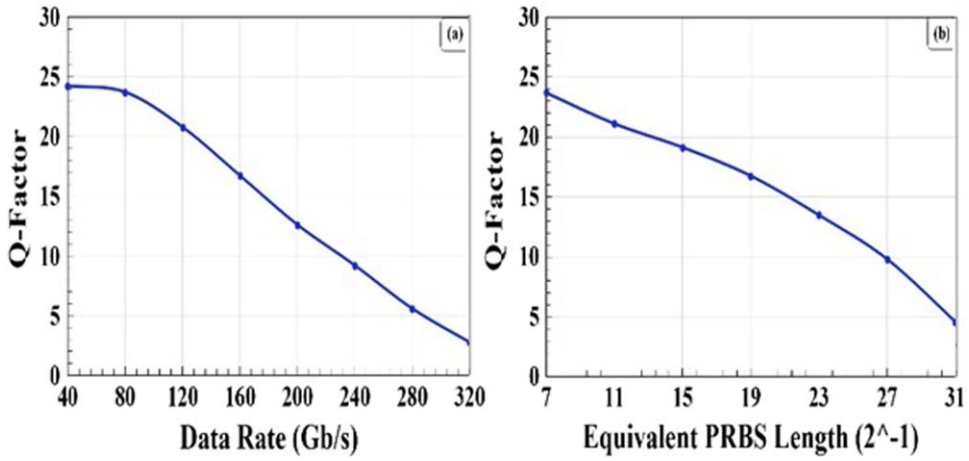

Figure 4. Q-factor of OR gate using two cascaded SOAs at 80 Gb s^{-1} versus (a) data rate and (a) equivalent PRBS length.

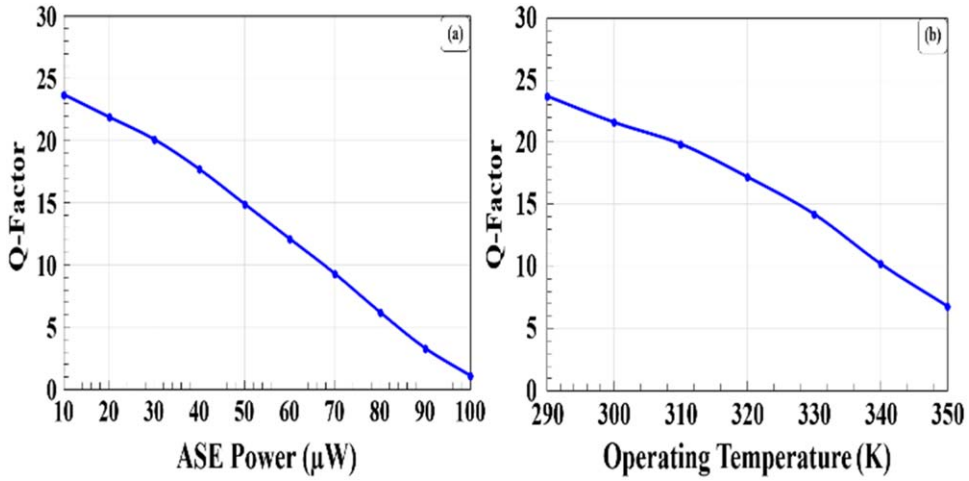

Figure 5. Q-factor of OR gate using two cascaded SOAs at 80 Gb s^{-1} versus (a) ASE power and (a) operating temperature.

response [19, 20]. Figure 4(b) shows that the Q-factor is also decreased with the increase of the equivalent PRBS length. The latter is defined as the maximum number of consecutive '1's, *r*, in this sequence whose binary word size is 2^r-1. The OR operation is stressed on the edge with increasing *r* as the risk of generating errors becomes higher due to the protracted strings of '0's- and '1's [21]. This explains the decrease in the Q-factor as the PRBS order, *r*, gets higher. Still, the proposed scheme achieves a more than acceptable Q-factor $=$ 9.8 for 27 bit-long equivalent PRBS length.

In the above results, an ideal SOA (i.e. $N_{SP} = 2$) operating at room temperature (~290 K) is considered. However, the amplified spontaneous emission (ASE) noise and operating temperature (T_{OP}) may also have a critical impact on performance, hence their influence should be taken into account, which is depicted in figures 5(a) and (b), respectively. In this study, the effects of ASE noise and T_{OP} on SOA1 and SOA2 are considered to be identical in order to simplify the calculations. The main noise contribution in SOAs is attributed to ASE [22], therefore, its effect cannot be neglected. Because ASE is accumulated, its effect on the whole scheme can become significant even if ASE from each SOA is small [23]. The ASE power is numerically added to the output powers of equations (9) and (10) using $P_{ASE} = N_{SP}(G_0-1)\,hfB_0$ [16], where the definition and values of these parameters are cited in table 1. The increase in ASE power causes an excessive increase in the mean power of bit '0' and thus results in a decrease in the Q-factor, as shown in figure 5(a). Despite this fact, we also notice from this figure that the two-cascaded SOAs-based OR logic gate is not significantly affected by the ASE and it achieves acceptable Q-factor even at relatively high values of ASE power. Another challenge, on the other hand, is finding SOAs that can efficiently operate at high temperatures, which is a topic worthy of studying. The effect of the SOAs' operating temperature is incorporated into this numerical analysis using the distribution equations of the quasi-Fermi levels described in detail in [24]. In figure 5(b), the Q-factor is decreased with

Table 2. Comparison of theoretically implemented OR gate at 80 Gb s^{-1} using different SOAs-based schemes.

Scheme	Data rate (Gb s^{-1})	Q-factor	Reference
SOA-DI	80	7	[3]
SOAs-MZI	80	11	[4]
Cascaded SOAs	80	23.7	This work

increasing T_{OP} and this happens due to several reasons. First, electrons are distributed over a wider range of energy at higher T_{OP} and therefore their number which is available for producing the device gain becomes smaller. Secondly, non-radiative recombination is increased at higher temperatures. Finally, the point of SOAs transparency is changed with a rise in temperature, which negatively affects the SOAs gain recovery time [25].

To fully assess the proposed scheme's performance, we compare it with previously reported AO OR logic gates theoretically implemented at 80 Gb s^{-1} using different SOA-based schemes [3, 4], as listed in table 2. We notice that the two-cascaded SOAs-based OR logic gate obtains a higher Q-factor at 80 Gb s^{-1} compared with other SOA-based schemes. It is expected that the data rate will be further increased with a higher Q-factor when exploiting two-photon absorption (TPA) or embedding quantum-dots [26] within the two-cascaded SOAs.

4. Conclusions

In this research, we have been able to theoretically show the merit of all-optical OR logic gate operation at 80 Gb s^{-1} with high performance using two properly cascaded and driven SOAs. The proposed OR logic gate has the potential of achieving Q-factor $=$ 9.2 at 240 Gb s^{-1} operating data rate, Q-factor $=$ 9.8 at 27 bit-long equivalent PRBS length, Q-factor $=$ 6.2 at 80 μW ASE power and Q-factor $=$ 6.2 at 340 K SOA operating temperature. We also found that the choice of the wavelength of the CW input signal is not so critical provided that it lies within the 1550–1570 nm range. We believe that the proposed scheme would be even more attractive when designed and employed in the context of integrated photonic circuits of enhanced functionality

Acknowledgments

Amer Kotb sincerely thanks the CAS President's International Fellowship Initiative (Grant No. 2019FYT0002) and the Talented Young Scientist Program in China for supporting this work.

Data availability statement

No new data were created or analysed in this study.

ORCID iDs

Amer Kotb https://orcid.org/0000-0002-3776-822X

References

[1] Willner A E, Fallahpour A, Alishahi F, Cao Y, Mohajerin-Ariaei A, Almaiman A, Liao P, Zou K, Willner A N and Tur M 2019 *J. Lightwave Technol.* **37** 21
[2] Willner A E, Khaleghi S, Chitgarha M R and Yilmaz O F 2014 *J. Lightwave Technol.* **32** 660
[3] Wang Q, Dong H, Sun H and Dutta N K 2006 *Opt. Commun.* **260** 81
[4] Kotb A, Zoiros K E and Guo C 2019 *J. Comp. Electron.* **18** 271
[5] Singh P, Tripathi D K, Jaiswal S and Dixit H K *Opt. Quantum Electron.* **46** 1435
[6] Hamie A, Sharaiha A and Guegan M 2003 *Microwave Opt. Technol. Lett.* **39** 39
[7] Mao Y, Liu B, Ullah R, Sun T and Zhao L 2020 *Opt. Commun.* **466** 125421
[8] Zhang X, Wang Y, Sun J and Liu D 2004 *Opt Express* **12** 361
[9] Zhang X, Zhao C, Liu H, Liu D and Huang D 2007 *Microwave Opt. Technol. Lett.* **49** 484
[10] Hamie A, Sharaiha A, Guegan M and Pucel B 2002 *IEEE Photon. Technol. Lett.* **14** 1439
[11] Kim J H, Oh K R, Kim H S and Cho K 2000 *IEEE Photon. Technol. Lett.* **12** 513
[12] Villafranca A, Garcés I, Cabezón M, Martínez J J, Izquierdo D and Pozo J 2010 Multiple-bit all-optical logic based on cross-gain modulation in a semiconductor optical amplifier *Proc. IEEE 12th Int. Conf. on Transparent Optical Networks*
[13] Pato S V, Meleiro R, Fonseca D, André P, Monteiro P and Silva H 2008 *IEEE Photon. Technol. Lett.* **20** 2078
[14] Fjelde T, Wolfson D, Kloch A and Janz C 2000 *Electron. Lett.* **36** 813

[15] Rizou Z V and Zoiros K E 2017 Semiconductor optical amplifier dynamics and pattern effects *Handbook of Optoelectronic Device Modeling and Simulation: Fundamentals, Materials, Nanostructures, LEDs, and Amplifiers* ed H Piprek (Boca Raton, FL: CRC Press) Ch. 25 pp 771
[16] Dutta N K and Wang Q 2013 *Semiconductor Optical Amplifiers* 2nd edn (Singapore: World Scientific)
[17] Kotb A, Zoiros K E and Guo C 2019 *J. Comp. Electron.* **18** 628
[18] Thapa S, Zhang X and Dutta N K 2019 *J. Mod. Opt.* **66** 100
[19] Zoiros K E, Chasioti R, Koukourlis C S and Houbavlis T 2007 *Optik* **118** 134
[20] Vardakas J S and Zoiros K E 2007 *Opt. Eng.* **46** 085005
[21] Siarkos T, Zoiros K E and Nastou D 2009 *Opt. Commun.* **282** 2729
[22] Shtaif M, Tromborg B and Eisenstein G 1998 *IEEE J. Quantum Electron.* **34** 869
[23] Kiyota M 2020 *IEEE J. Quantum Electron.* **56** 2200210
[24] Connelly M J 2004 *Semiconductor Optical Amplifiers* (New York: Kluwer Academic Publisher) ch 4
[25] Kumar Y and Shenoy M R 2016 *Pramana J. Phys.* **87** 1
[26] Kotb A, Zoiros K E and Guo C 2019 *Opt. Laser Technol.* **112** 442